Spring 4-2016

Predictive Formula for Electron Range over a Large Span of Energies

Anne C. Starley
Utah State University

Gregory Wilson
Utah State University

Lisa Montierth Phillipps
Utah State University

JR Dennison
Utah State Univesity

Predictive Formula For Electron Range over a Large Span of Energies

Anne Starley, Gregory Wilson, Lisa Phillipps, and JR Dennison

USU Materials Physics Group

Utah State University, Logan, UT 84332-4414

I. Introduction to Range

The range, commonly known as the penetration depth, describes the maximum distance electrons can travel through a material, given an initial incident energy, before they lose all of their kinetic energy and come to a rest.[1,2] The primary energy loss mechanism which causes the electron to lose its kinetic energy is due to inelastic collisions within material. Due to the probabilistic nature of this mechanism, the Continuous Slow Down Approximation (CSDA) is often employed to simplify the problem where the stopping power is taken as a constant.

This idea is illustrated by a Lichtenburg discharged tree pictured in Fig. 1. This "tree" demonstrates a situation where accelerated high energy electrons comes to rest and deposit charge at a given range in an insulating material.[3] The side view of the Lichtenburg tree displays the melted plastic caused by the energy of the deposited incident electrons at a uniform penetration depth. Here the stored charge is dissipated through a discharge.[1]

Fig. 1. Front (Left) and side (Right) views of a Lichtenberg discharge tree. The white line (Right) indicates the narrow distribution of deposited charge from a ~1 MeV electron beam at R≈3 mm in a PMMA sample.

II. Original Model

The previously developed model predicts the energy-dependent range, R(E), as a function of incident electron energy for materials found in the NIST ESTAR database. In a continuous composite analytic approximation to the range with a *single fitting parameter, N_V,* spanning incident energies, *E*, from <10 eV to >10 MeV, the following functions (Eqs. 2, 3, and 4) describe the energy-dependent range, ***R(E),*** in terms of N_V and material parameters mass density ρ_m, effective atomic number and weight N_A and M_A and band gap E_{gap}.[1]

$$R(E;N_V)=\begin{cases}\left[\frac{E}{E_m}\right]\frac{\lambda_{IMFP}(E_m)(1-exp[-1])}{\left(1-exp\left[-\frac{E}{E_m}\right]\right)^2} & ;E<E_m\\ \left[\frac{E}{E_m}\right]\frac{\lambda_{IMFP}(E)}{1-exp\left[-\frac{E}{E_m}\right]} & ;E_m\le E\le E_{HI}\\ bE^n\left(1-\left[1+\left[\frac{E/N_V}{m_ec^2}\right]\right]^{-2}\right) & ;E>E_{HI}\end{cases}$$

Eq. (1). Range for low, medium, and high energy regimes.

$$E_m=2.8\left[E_{gap}^2+E_p^2\right]^{\frac{1}{2}}$$

Eq. (2). Mean energy lost per collision.

$$E_p=\hbar\left(\frac{N_VN_A\rho_mq_e^2}{m_e\varepsilon_0M_A}\right)^{\frac{1}{2}}$$

Eq. (3). Plasmon energy.

Manual fits to these range equations and optimum values of N_V were found using data for about 20 well-known elements and compounds with range data from the ESTAR database.[2] Fig. 2 shows several approximate fits to the range data.

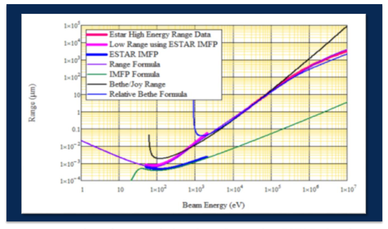

Fig. 2. Comparison between several range approximations and the data from the ESTAR database for Au. The IMFP data for Au are also plotted along with the TPP-2M IMFP formula for $\lambda_{IMFP}(E)$.

III. Predictive Formula for N_V

A simple formula [Eq. (4)] was found to predict our single range parameter, N_v, as a function of only mean atomic number derived from the stoichiometric formula. This simple formula resulted from extensive analysis of much more complex predictive formula for N_V involving sums of power law terms for density, effective atomic number and weight, and bandgap plus other properties including plasmon energy, conductivity, phase, and more. This general fit for N_V was evaluated using general least squares fit analysis methods to simultaneously determine the best estimates for fitting parameters for each material property. Amazingly, the simple formula Eq. (4) involving only Z_m was the result.

Fig. 3 and Table 1 show the results of the fits with Eq. (4) for A,B and C. The fitting parameters was then used to calculate an estimate of N_v using the power law model. Plotting this estimate of N_v versus the true value of N_v Goodness of fit metrics χ^2_{Nv} and R allows quantification of the quality of the fits.

To refine Eq. (4), separate fits were made for materials subcategorized into grouping such as insulators, semiconductors, and conductors [see Figs. 3(b-d)] and solids, liquids, and gasses with the hope that this categorization might unearth additional information. Semiconductor show excellent agreement. Insulators show very good agreement, with a slight downward concavity. Although conductors show good agreement, it is apparent that an additional higher order correction for conductors needed is needed to account for electron overlap in the d and f orbitals of transition and rare earth/actinide elements.

$$N_V(Zm)=AZ_m{}^B-C$$

Eq. (4). Predictive formula for effective number of valence electrons, where Z_m the is mean atomic number and *A*, *B*, and *C* are constants found through fits shown in Fig. 3.

Table 1. Constants and Goodness of fit predictive N_V fits.

Materials	A	B	C	χ^2_{Nv}	R
All	20.196	0.653	21.727	0.006	0.99
Insulators	21.581	0.730	22.892	0.0032	0.99
Conductors	22.898	0.604	24.982	0.0053	0.99
Semiconductors	14.817	0.153	16.585	0.0055	0.99

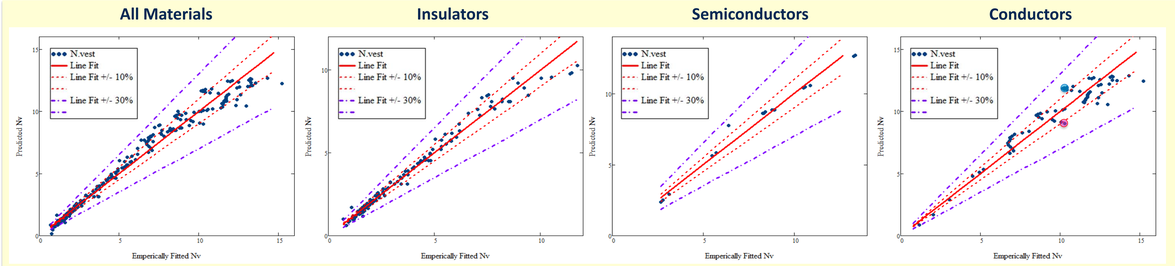

Fig. 3. The graphs examine N_V found from fits to the NIST database data versus N_V predicted using Eq. (4). Nominally, for exact agreement the slope of the fit would be 1 with an intercept of 0 and χ^2_{Nv} approaching 0. 10% and 30% error lines to the slope are marked in dashed red and dashed purple lines, respectively. Values for the constants for predictive N_V from Eq. (4) and the goodness of linear fit for Fig. (3) graphs are found in Table 1.

IV. Accuracy of Range for Predicted N_V

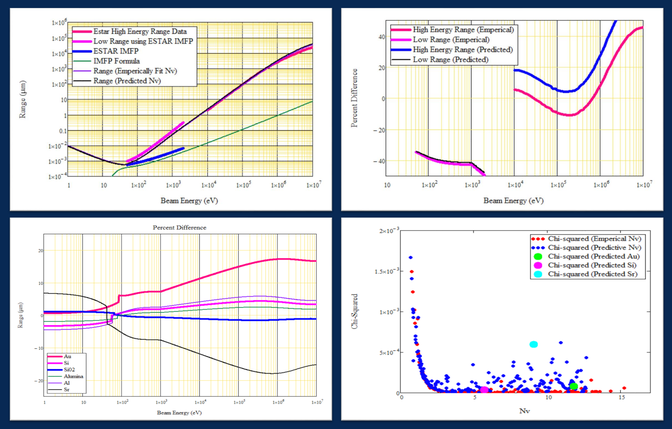

Fig. 4. (a) Strontium range calculated using both empirical and predicted N_V values as compared to ESTAR range data. (b) Percent differences for both medium and high energy regimes for Sr range calculated ranges for both empirical and predicted N_V values as compared to ESTAR range and inelastic mean free path data. (c) Percent differences between ranges calculated with empirical and predicted N_V values for SiO_2, Al_2O_3, Si, Al, Au and Sr. (d) χ^2 values for comparison of ESTAR range data to ranges calculated for both the empirical and predicted N_V values for all materials in the NIST material database (see Table 3). The χ^2 values for Si, Au and Sr with predicted N_V are highlighted, illustrating their extreme variances from the empirical data.

Range values as a function of energy predicted with empirical NV values derived from fits to the NIST database range and inelastic mean free path values were found to give good fits with differences typically less (often much less) than ±20% over full 10 eV<*E*<10 MeV spans.[1] Fig. 4(a) shows such a plot for one of the worst fit materials, Sr [see in Fig. 3(d) and Fig. 4(b) and Table 2].

To better gauge the validity of the predictive formula for N_V, Eq. (4), comparisons are made of ranges calculated with both empirical and predicted N_V values (found in Table 3). Comparisons are shown in Figs. 4(b) and 4(c) for five different materials [including two materials with the highest inconsistency between the two data sets--strontium (Sr) and gold (Au)]. Agreement between the ranges calculated with predicted N_V values and ESTAR range data are shown Fig. 4(d) for all 249 materials in Table 3.

Table 2. Differences in the empirical and predicted N_V for various materials.

Material	Empirical N_V	Predicted N_V	Percent Error
SiO_2	4.716	4.646	1.5%
Al_2O_3	4.538	4.652	2.5%
Si	5.493	5.702	3.7%
Al	5.195	5.468	5.1%
Au	10.814	11.800	9%
Sr	10.074	9.071	10%

V. Materials with Predicted Ranges

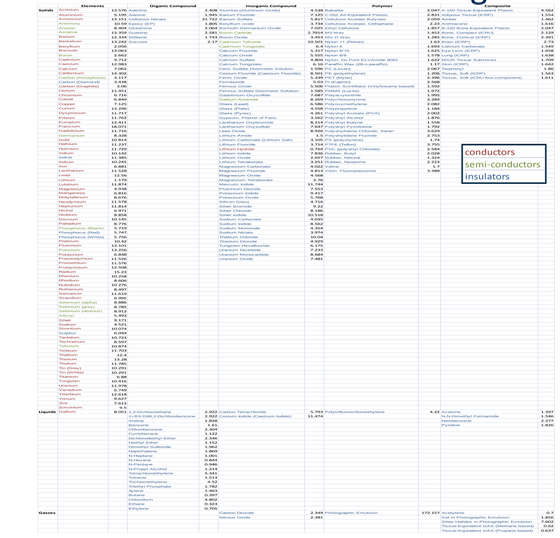

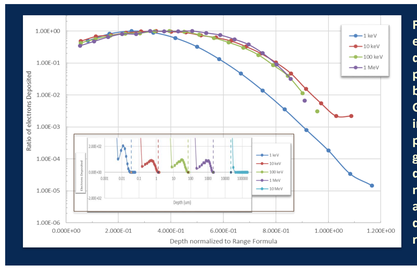

Fig. 5. (inset) Number of electrons deposited versus depth of electron penetration in Al for several beam energies using GEANT4. The dotted lines indicate CSDA range as predicted by Eq. (1). (Main graph) Fraction of electrons deposited normalized by the maximum deposition fraction as a function of penetration depth scaled by the CSDA range.

The fraction of electrons deposited as a function of penetration depth can be calculated with advanced simulation programs such as GEANT4, as shown in the inset of Fig. 5. Fig. 5 shows the fraction of electrons deposited normalized by the maximum deposition fraction as a function of penetration depth scaled by the CSDA range. The dotted lines indicate CSDA range as predicted by Eq. (1). Note for energies of 10 keV and above, where GEANT4 simulations are valid, the scaled curves are the same with a deposition fraction ~0.2% at the CSDA range. This suggests that the single mean ranges for energy in our CSDA approximation can be broadened by convolution with this universal curve to predict approximate internal charge deposition curves for a wide span of energies for any material using our composite formula for the range and predictive formula for N_V.

VI. Future Work

- We will create an online range prediction calculator that will be able to produce the range of a material with only input of the common material parameters mass density ρ_m, effective atomic number and weight N_A and M_A from the stoichiometric formula (or relative amounts of elements in compounds and composites), and band gap E_{gap} (or HOMO-LUMO gap).
- We propose to develop a better relativistic approximation for Eq. (1) to improve range predictions above m_ec^2=0.5 MeV.
- We prose to improve N_V predictions by adding addition Z_m dependence in Eq. (4).
- Gas and liquid materials do not have band gaps, a necessary parameter in our range model. The HOMO-LUMO energy gaps may be an appropriate surrogate. We will study the HOMO-LUMO gap and its potential connection to the range.

VII. References

1. Wilson, G., & Dennison, J.R. (2010). *Approximation of range in materials as a function of incident electron energy.*
2. Teancum Quist (with Greg Wilson and JR Dennison), "Compilation and Comparison of Electron Penetration Ranges as a Function of Effective Number of Valence Electrons," Utah State University, Logan, UT, April 2013.
3. Starley, A., Phillipps, L., Wilson, G., Dennison, J.R., *Predictive Formula For Electron Range Over A Large Span of Energies* APS Four Corners Poster presented at APS Four Corners Meeting 2015,Arizona State University, Mesa, AZ, 2015.
4. Meloy, R., private communications, 2016.

We gratefully acknowledge contributions from other members of the Materials Physics Groups. This work was supported by USU URCO fellowships and a NASA Space Technology Research Fellowship.

Scan code to access the USU Material Physics Group papers and presentations.